

# Electric charge fluctuations in central Pb+Pb collisions at 20, 30, 40, 80 and 158 AGeV

The NA49 Collaboration

*Results are presented on event-by-event electric charge fluctuations in central Pb+Pb collisions at 20, 30, 40, 80 and 158 AGeV. The observed fluctuations are close to those expected for a gas of pions correlated by global charge conservation only. These fluctuations are considerably larger than those calculated for an ideal gas of deconfined quarks and gluons. The present measurements do not necessarily exclude reduced fluctuations from a quark-gluon plasma because these might be masked by contributions from resonance decays.*

C. Alt<sup>9</sup>, T. Anticic<sup>21</sup>, B. Baatar<sup>8</sup>, D. Barna<sup>4</sup>, J. Bartke<sup>6</sup>, M. Behler<sup>13</sup>, L. Betev<sup>9</sup>, H. Białkowska<sup>19</sup>, A. Billmeier<sup>9</sup>, C. Blume<sup>7</sup>, B. Boimska<sup>19</sup>, M. Botje<sup>1</sup>, J. Bracinik<sup>3</sup>, R. Bramm<sup>9</sup>, R. Brun<sup>10</sup>, P. Bunčić<sup>9,10</sup>, V. Cerny<sup>3</sup>, P. Christakoglou<sup>2</sup>, O. Chvala<sup>15</sup>, J.G. Cramer<sup>17</sup>, P. Csató<sup>4</sup>, N. Darmenov<sup>18</sup>, A. Dimitrov<sup>18</sup>, P. Dinkelaker<sup>9</sup>, V. Eckardt<sup>14</sup>, P. Filip<sup>14</sup>, D. Flierl<sup>9</sup>, Z. Fodor<sup>4</sup>, P. Foka<sup>7</sup>, P. Freund<sup>14</sup>, V. Friese<sup>7</sup>, J. Gál<sup>4</sup>, M. Gaździcki<sup>9</sup>, G. Georgopoulos<sup>2</sup>, E. Gładysz<sup>6</sup>, K. Grebieszko<sup>20</sup>, S. Hegyi<sup>4</sup>, C. Höhne<sup>13</sup>, K. Kadija<sup>21</sup>, A. Karev<sup>14</sup>, M. Kliemant<sup>9</sup>, S. Kniege<sup>9</sup>, V.I. Kolesnikov<sup>8</sup>, T. Kollegger<sup>9</sup>, E. Kornas<sup>6</sup>, R. Korus<sup>12</sup>, M. Kowalski<sup>6</sup>, I. Kraus<sup>7</sup>, M. Kreps<sup>3</sup>, M. van Leeuwen<sup>1</sup>, P. Lévai<sup>4</sup>, L. Litov<sup>18</sup>, B. Lungwitz<sup>9</sup>, M. Makariev<sup>18</sup>, A.I. Malakhov<sup>8</sup>, C. Markert<sup>7</sup>, M. Mateev<sup>18</sup>, B.W. Mayes<sup>11</sup>, G.L. Melkumov<sup>8</sup>, C. Meurer<sup>9</sup>, A. Mischke<sup>7</sup>, M. Mitrovski<sup>9</sup>, J. Molnár<sup>4</sup>, St. Mrówczyński<sup>12</sup>, G. Pála<sup>4</sup>, A.D. Panagiotou<sup>2</sup>, D. Panayotov<sup>18</sup>, A. Petridis<sup>2</sup>, M. Pikna<sup>3</sup>, L. Pinsky<sup>11</sup>, F. Pühlhofer<sup>13</sup>, J.G. Reid<sup>17</sup>, R. Renfordt<sup>9</sup>, A. Richard<sup>9</sup>, C. Roland<sup>5</sup>, G. Roland<sup>5</sup>, M. Rybczyński<sup>12</sup>, A. Rybicki<sup>6,10</sup>, A. Sandoval<sup>7</sup>, H. Sann<sup>7</sup>, N. Schmitz<sup>14</sup>, P. Seyboth<sup>14</sup>, F. Siklér<sup>4</sup>, B. Sitar<sup>3</sup>, E. Skrzypczak<sup>20</sup>, G. Stefanek<sup>12</sup>, R. Stock<sup>9</sup>, H. Ströbele<sup>9</sup>, T. Susa<sup>21</sup>, I. Szentpétery<sup>4</sup>, J. Sziklai<sup>4</sup>, T.A. Trainor<sup>17</sup>, D. Varga<sup>4</sup>, M. Vassiliou<sup>2</sup>, G.I. Veres<sup>4</sup>, G. Vesztergombi<sup>4</sup>, D. Vranić<sup>7</sup>, A. Wetzler<sup>9</sup>, Z. Włodarczyk<sup>12</sup>, I.K. Yoo<sup>16</sup>, J. Zaranek<sup>9</sup>, J. Zimányi<sup>4</sup>

<sup>1</sup>NIKHEF, Amsterdam, Netherlands.

<sup>2</sup>Department of Physics, University of Athens, Athens, Greece.

<sup>3</sup>Comenius University, Bratislava, Slovakia.

<sup>4</sup>KFKI Research Institute for Particle and Nuclear Physics, Budapest, Hungary.

<sup>5</sup>MIT, Cambridge, USA.

<sup>6</sup>Institute of Nuclear Physics, Cracow, Poland.

<sup>7</sup>Gesellschaft für Schwerionenforschung (GSI), Darmstadt, Germany.

<sup>8</sup>Joint Institute for Nuclear Research, Dubna, Russia.

<sup>9</sup>Fachbereich Physik der Universität, Frankfurt, Germany.

<sup>10</sup>CERN, Geneva, Switzerland.

<sup>11</sup>University of Houston, Houston, TX, USA.

<sup>12</sup>Institute of Physics Świ etokrzyska Academy, Kielce, Poland.

<sup>13</sup>Fachbereich Physik der Universität, Marburg, Germany.

<sup>14</sup>Max-Planck-Institut für Physik, Munich, Germany.

<sup>15</sup>Institute of Particle and Nuclear Physics, Charles University, Prague, Czech Republic.

<sup>16</sup>Department of Physics, Pusan National University, Pusan, Republic of Korea.

<sup>17</sup>Nuclear Physics Laboratory, University of Washington, Seattle, WA, USA.

<sup>18</sup>Atomic Physics Department, Sofia University St. Kliment Ohridski, Sofia, Bulgaria.

<sup>19</sup>Institute for Nuclear Studies, Warsaw, Poland.

<sup>20</sup>Institute for Experimental Physics, University of Warsaw, Warsaw, Poland.

<sup>21</sup>Rudjer Boskovic Institute, Zagreb, Croatia.

*Keywords:* Relativistic heavy-ion collisions; Charge fluctuations; QGP;

## I. INTRODUCTION

Ultra-relativistic heavy-ion collisions provide the opportunity to study the properties of strongly interacting matter. One of the predicted features of this matter, which one hopes to establish in heavy-ion collisions, is the occurrence of a phase transition between a purely hadronic state and the quark-gluon plasma. Recently several results were reported [1, 2] which suggest that this transition starts in central Pb+Pb collisions at energies around 30 AGeV [3, 4]. The search for further signals of deconfinement is in progress and may provide additional support for such an interpretation. Among them a suppression of event-by-event fluctuations of electric charge was predicted [5, 6] as a consequence of deconfinement. Estimates of the magnitude of the charge fluctuations indicate that they are much smaller in a quark-gluon plasma than in a hadron gas. Thus, naively, a decrease of the fluctuations is expected when the collision energy crosses the threshold for the deconfinement phase transition. However, this prediction is derived under the assumptions that the initial fluctuations survive hadronization and that their relaxation times in hadronic matter are significantly longer than the hadronic stage of the collision [5, 6, 7]. First data on charge fluctuations in central heavy ion collisions were published by PHENIX [8] and STAR [9] at the BNL RHIC, and preliminary results at the CERN SPS were shown by NA49 [10]. The predicted large suppression of charge fluctuations was not observed. Results by NA49 on transverse momentum and strangeness fluctuations can be found in Refs. [11, 12] and [13, 14], respectively.

In this work final results on electric charge fluctuations in central Pb+Pb collisions at 20, 30, 40, 80 and 158 AGeV measured by NA49 at the CERN SPS are presented and discussed in view of their significance as a signal of deconfinement. The used measure of charge fluctuations  $\Delta\Phi_q$  [15] is introduced in Sec. II. The experimental set-up is presented in Sec. III and the data sets as well as analysis method are described in Sec. IV. Results are given in Sec. V and are discussed in Sec. VI. The summary is given in Sec. VII.

## II. THE MEASURE OF CHARGE FLUCTUATIONS

The magnitude of the measured charge fluctuations depends not only on the unit of electric charge carried by degrees of freedom of the system (hadrons or quarks and gluons),

but depends also on trivial effects, which may obscure the physics of interest. The two most important of these effects are the fluctuations in the event multiplicity, caused mostly by the variation of the impact parameter, and changes in the mean multiplicity due to changes of the acceptance in which fluctuations are studied. In addition to the  $\tilde{D}$  measure of charge fluctuations [5] several alternative measures such as  $\nu_{+-,dyn}$ , [16] and  $\Delta\Phi_q$  [15] were proposed to minimize the sensitivity to these effects. In this analysis we use  $\Delta\Phi_q$  which is constructed from the well established measure  $\Phi$  of event-by-event fluctuations, defined as [18]:

$$\Phi = \sqrt{\frac{\langle Z^2 \rangle}{\langle N \rangle}} - \sqrt{\overline{z^2}}, \quad (1)$$

where:

$$z = x - \bar{x}, \quad Z = \sum_{i=1}^N (x_i - \bar{x}). \quad (2)$$

In these equations  $x$  denotes a single particle variable,  $N$  is the number of particles of the event within the acceptance, and over-line and  $\langle \dots \rangle$  denote averaging over a single particle inclusive distribution and over events, respectively. By construction, for a system which is an independent sum of identical sources of particles the value of  $\Phi$  is equal to the value of  $\Phi$  for a single source and does not depend on the number of superimposed sources [18, 19]. In this analysis  $x$  in Eqs. (2) is taken to be the electric charge  $q$  and the measure is called  $\Phi_q$ .

For a scenario in which particles are correlated only by global charge conservation (GCC) the value of  $\Phi_q$  is given by [15, 17]:

$$\Phi_{q,GCC} = \sqrt{1 - P} - 1, \quad (3)$$

where

$$P = \frac{\langle N_{ch} \rangle}{\langle N_{ch} \rangle_{tot}} \quad (4)$$

with  $\langle N_{ch} \rangle$  and  $\langle N_{ch} \rangle_{tot}$  being the mean charged multiplicity in the detector acceptance and in full phase space (excluding spectator nucleons), respectively. Strictly speaking Eq. (3) holds for vanishing net charge. However, as shown in [17], Eq. (3) serves as a good approximation also for realistic non-zero values of the total net charge.

In order to remove the sensitivity to GCC the measure  $\Delta\Phi_q$  is defined as the difference:

$$\Delta\Phi_q = \Phi_q - \Phi_{q,GCC} . \quad (5)$$

By construction, the value of  $\Delta\Phi_q$  is zero if the particles are correlated by global charge conservation only. It is negative in case of an additional correlation between positively and negatively charged particles, and it is positive if the positive and negative particles are anti-correlated [15].

### III. EXPERIMENTAL SET-UP

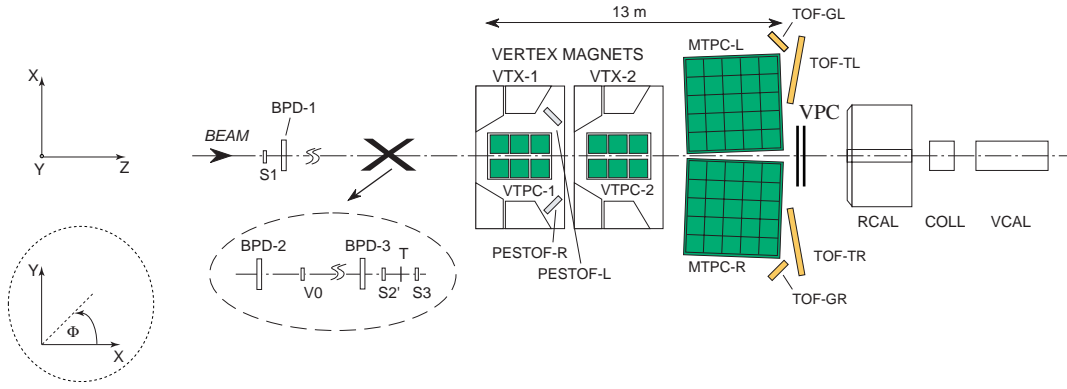


FIG. 1: The experimental set-up of the NA49 experiment.

The NA49 experimental set-up [20] is shown in Fig. 1. The main detectors of the experiment are four large-volume Time Projection Chambers (TPCs). Two of these, the Vertex TPCs (VTPC-1 and VTPC-2), are located in the magnetic field of two superconducting dipole magnets. This allows separation of positively and negatively charged tracks and a measurement of the particle momenta. The nominal magnetic field is adjusted in proportion to the beam energy to ensure a good acceptance at all energies. The other two TPCs (MTPC-L and MTPC-R), positioned downstream of the magnets, are optimized for precise measurement of the ionization energy loss  $dE/dx$  which is used for the determination of the particle masses. Additional information on the particle masses is provided by two Time-of-Flight (TOF) detector arrays which are placed behind the MTPCs. The centrality of the collisions is determined by a calorimeter (VCAL) which

measures the energy of the projectile spectators. To cover only the spectator region the geometrical acceptance of the VCAL was adjusted for each beam energy by a proper setting of a collimator (COLL) [20, 21]. The Beam Position Detectors (BPD-1, BPD-2 and BPD-3) are used to determine the  $x$ - and  $y$ -coordinate of the beam at the target. Alternatively the main vertex position is reconstructed as the common intersection point of reconstructed tracks. A detailed description of the NA49 set-up and tracking software can be found in Ref. [20].

## IV. DATA ANALYSIS

### A. Data

At all energies 50K events were analyzed with a centrality of 7% of the inelastic cross-section except at 158 AGeV where the 10% most central events were selected.

To minimize the contributions of non-target collisions only events which satisfy the following two selection criteria were used in the analysis. Firstly, the reconstruction of the primary vertex position based on BPD and TPC data had to be successful. Secondly, the difference between vertex coordinates resulting from the BPD and TPC data should be smaller than  $\pm 1$  mm in  $x$ - and  $y$ -coordinate and  $\pm 5$  mm in  $z$ -coordinate.

Several quality criteria were applied to the particle tracks. All tracks should contain points measured in at least one of the Vertex TPCs and the number of all measured points,  $n_P$ , should be larger than 30. Only for these particles charge and momentum determination is considered to be reliable. To avoid double counting of particles only tracks with a measured number of points larger than 50% of all geometrically possible points were accepted. The number of particles originating from weak decays and secondary interactions is reduced by only using tracks for which the  $x$ - and  $y$ -position extrapolated to the  $z$ -coordinate of the target is close to the position of the interaction point ( $|b_x| < 2$  cm for the  $x$ - and  $|b_y| < 1$  cm for the  $y$ -coordinate).

Furthermore particles are required to lie in a well defined acceptance region in  $y$ ,  $p_T$  and  $\phi$  ( $y$  is the rapidity in the center-of-mass system calculated assuming the pion mass,  $p_T$  is the transverse momentum and  $\phi$  denotes the azimuthal angle). A well defined acceptance is essential for comparison of the results with model predictions and with data from other

experiments. The acceptance limits are parametrized by the function:

$$p_T(y, \phi) = \frac{1}{A(y) + \left(\frac{D(y)+\phi}{C(y)}\right)^6} + B(y), \quad (6)$$

where  $A(y)$ ,  $B(y)$ ,  $C(y)$  and  $D(y)$  are parameters depending on the rapidity and collision energy. The values of the parameters for positively charged tracks in the nominal magnetic field ( $B_y$  pointing upward) are given in Table 1. These parameters also apply to negative tracks or to a reversed magnetic field ( $B_y$  pointing downward) provided  $\phi$  in Eq. (6) is replaced by  $\phi' = \text{sign}(\phi)(180 - |\phi|)$ .

As an example we show in Fig. 2 the acceptance in  $p_T$ ,  $\phi$  used for the analysis for  $-0.2 < y < 0$  and  $1.4 < y < 1.6$  at 20 AGeV and  $-0.6 < y < -0.4$  and  $1.4 < y < 1.6$  at 158 AGeV.

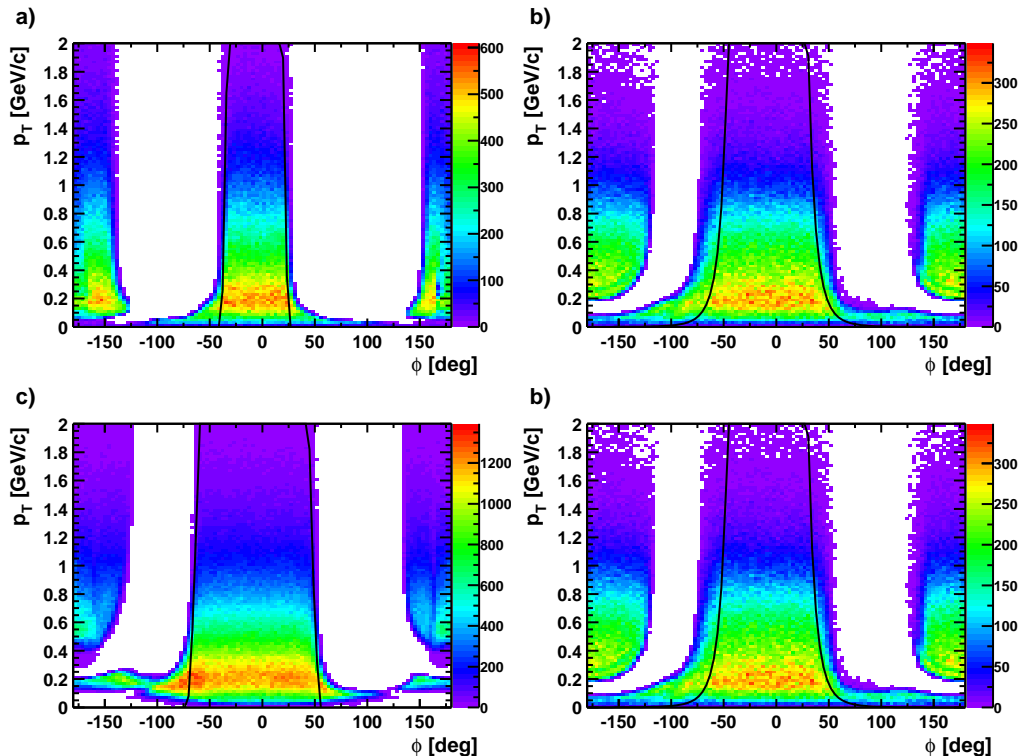


FIG. 2: Distributions of registered particles in the  $p_T$ - $\phi$ -plane for  $-0.2 < y < 0$  (a) and  $1.4 < y < 1.6$  (b) at 20 AGeV and  $-0.6 < y < -0.4$  (c) and  $1.4 < y < 1.6$  (d) at 158 AGeV. The acceptance limits used in the analysis are shown by the solid lines.



TABLE I: Values of the parameters  $A$ ,  $B$ ,  $C$  and  $D$  of the acceptance limits, Eq. 6, for different energies and rapidities. The dimensions of the parameters are such that the use of the  $\phi$  angle in degrees and the rapidity in the center-of mass system results in the  $p_T$  limit in GeV/ $c$ .

$y$	20AGeV				30AGeV				40AGeV				80AGeV				158AGeV			
	A	B	C	D	A	B	C	D	A	B	C	D	A	B	C	D	A	B	C	D
-0.5									0	0	23	4	0	0	35	-10	0	-1	63	-8
-0.3					0	0	25	-7	0	0	30	7	0	0.07	40	-10	0	0	57	-10
-0.1	0	-1	32	-7	0	0	31	-8	0	0	38	10	0	0.07	46	-10	0	0.09	63	-13
0.1	0	0	34	-8	0	0	40	-8	0	0	43	8	0	0.05	52	-12	0	0.08	67	-4
0.3	0	0	41	-8	0	0	44	-8	0	0	46	7	0	0	58	-7	0	0.08	65	-3
0.5	0	-0.05	47	-8	0	0	46	-7	0	0	40	0	0	-1	29	-2	0	0.05	27	0
0.7	0	-0.1	50	-7	0	0	42	0	0	0	22	0	0	0.05	26	0	0	0	35	0
0.9	0	-0.3	53	-3	0	0	35	-10	0	0	34	6	0	0.08	35	0	0	0.1	41	0
1.1	0	-0.2	38	-10	0	0	39	-13	0	0	46	15	0.3	0.1	67	-27	0.34	0.43	109	0
1.3	0	-0.1	42	-12	0	0	44	-14	0	0	52	15	0.3	0.3	75	-15	0.36	0.43	100	0
1.5	0	0	43	-8	0	0	55	-21	0	0.1	58	20	0.3	0.27	85	0	0.55	0.4	100	0
1.7	0	0	51	-18	0	0.08	62	-2	0	0.08	72	0	0.3	0.18	75	0	0.6	0.4	88	0
1.9	0	0	63	-4	0	0.08	67	0	0	0.08	68	0	0.45	0.15	70	0	0.61	0.35	73	0
2.1	0	0	62	0	0	0.05	61	0	0	0.09	60	0	0.5	0.12	50	0	0.73	0.34	55	0
2.3	0	0	57	0	0.6	0.05	57	0	0.5	0.08	50	0	0.75	0.08	50	0	1.7	0.28	60	0
2.5	0.7	0	54	0	0.6	0	46	0	0.6	0.05	40	0	2.2	0.08	50	0	2.8	0.25	60	0
2.7	0.7	0	41	0	1	0	33	0	1.5	0.05	35	0	3.2	0.08	45	0	5	0.2	57	0
2.9	1.5	0	30	0	2.7	0	32	0					4.5	0.08	45	0	7	0.15	60	0
3.1													5.5	0	45	0	7	0.1	70	0

## B. Analysis

Charge fluctuations are studied as a function of the width of the rapidity interval  $\Delta y$ . These rapidity intervals were centered around 1.27, 1.07, 0.89, 0.89 and 0.89 for the 20,

30, 40, 80 and 158 AGeV data, respectively. The measures  $\Phi_q$  and  $\Delta\Phi_q$  were calculated for ten different rapidity intervals increasing in size from  $\Delta y = 0.3$  to  $\Delta y = 3$  in equal steps and will be plotted either versus  $\Delta y$  or the corresponding ratio  $\langle N_{ch} \rangle / \langle N_{ch} \rangle_{tot}$ . The largest rapidity interval contains approximately 90% of all accepted particles. In Fig. 3 the rapidity distribution of the accepted particles at 158 AGeV is shown together with the largest rapidity interval used in the analysis.

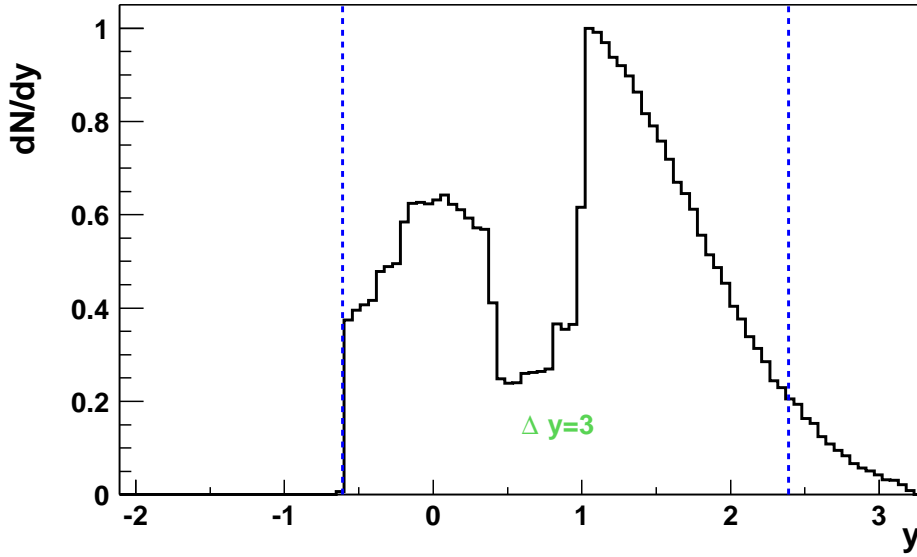


FIG. 3: The rapidity distribution of accepted particles in central Pb+Pb collisions at 158 AGeV. The largest rapidity interval used for the analysis is indicated by dashed lines.

For each event the positively and negatively charged particles which fall into each rapidity interval and the corresponding  $p_T$ - $\phi$  acceptance are counted and using these numbers ( $N_+$  and  $N_-$ ) the values of  $\Delta\Phi_q$  are calculated. The total charged particle multiplicity,  $\langle N_{ch} \rangle_{tot}$ , was estimated for each energy based on the NA49 measurements [1, 2].

### C. Errors

The statistical error of  $\Delta\Phi_q$  is calculated by dividing the whole sample of events into 10 subsamples and calculating  $\Delta\Phi_q$  for each subsample separately. The dispersion of the obtained  $\Delta\Phi_q$  values divided by  $\sqrt{9}$  has been taken as the statistical error. The systematic errors of  $\Delta\Phi_q$  are estimated by varying track quality cuts: The values of  $\Delta\Phi_q$  are calculated for two additional sets of cuts, more ( $n_P = 35, |b_x| < 0.75$  cm and  $|b_y| < 0.5$  cm) and less ( $n_P = 30, |b_x| < 4.5$  cm and  $|b_y| < 2.5$  cm) restrictive in comparison to the standard cuts. The accepted particle multiplicity decreases by about 25% when changing from less to more restrictive cuts. The difference of these two  $\Delta\Phi_q$  values is considered as the systematic error. Since the statistical errors are much smaller only the systematic errors are shown in the figures.

## V. RESULTS

A simple measure of charge fluctuations is the width of the distribution of net-charge  $Q = N_+ - N_-$  in the events. As an example the distribution for central Pb+Pb collisions at 158 AGeV is shown in Fig. 4. This distribution is compared to the net-charge distribution obtained from mixed events (dashed line in Fig. 4) constructed by randomly selecting particles from different events according to the multiplicity distribution measured for the data. The net-charge distribution from mixed events is significantly broader than the net-charge distribution obtained from real events.

The main source of the observed difference is charge conservation which correlates positively and negatively charged particles in the real, but not in the mixed events. This is demonstrated in Fig. 5 where the  $\Phi_q$  values are plotted as a function of the fraction of accepted particles  $\langle N_{ch} \rangle / \langle N_{ch} \rangle_{tot}$  for central Pb+Pb collisions at 20-158 AGeV. The main trend observed in the data, a monotonic decrease with increasing fraction of accepted particles, is approximately reproduced by introducing global charge conservation as the only source of particle correlations (Eq. 3 shown by the dashed line in Fig. 5).

By construction, the previously introduced measure  $\Delta\Phi_q$  is insensitive to the correlations due to global charge conservation (see Sec. II). The dependence of  $\Delta\Phi_q$  on the width of the rapidity interval  $\Delta y$  is shown in Fig. 6 for central Pb+Pb collisions at 20, 30, 40, 80

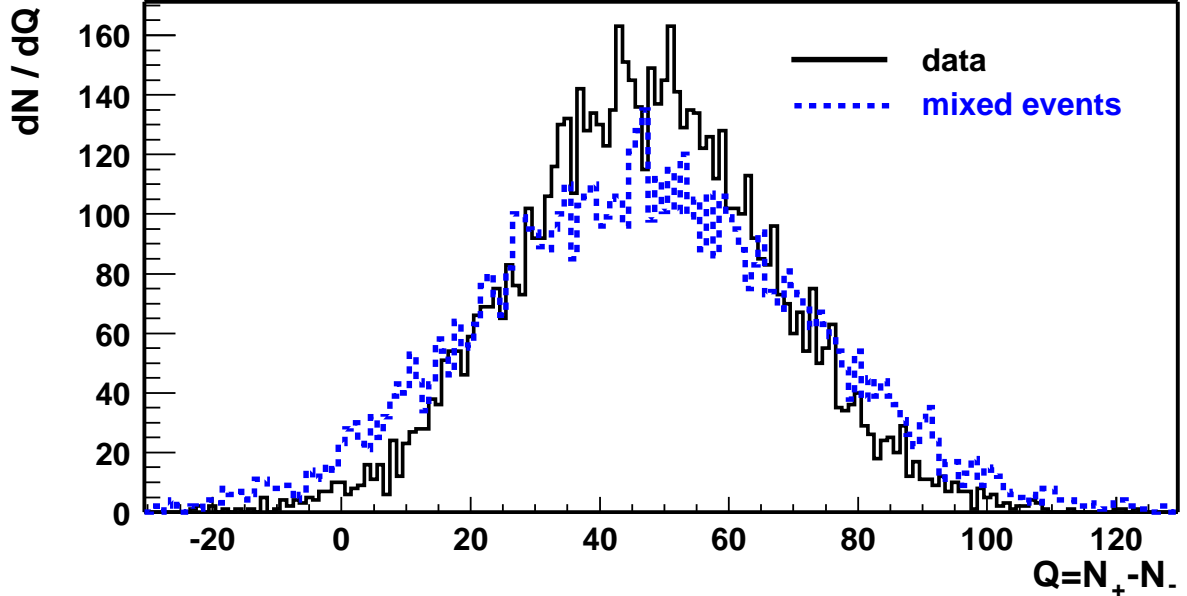


FIG. 4: The distribution of the net-charge for central Pb+Pb collisions at 158 AGeV (solid line) and the corresponding distribution obtained for mixed events (dotted line) in the maximum rapidity interval  $\Delta y = 3$ .

and 158 AGeV. The study of charge fluctuations as a function of  $\Delta y$  was suggested in the original proposal [5, 6]. The measured values of  $\Delta\Phi_q$  vary between 0 and  $-0.05$ . They are significantly larger than the values expected for QGP fluctuations ( $-0.5 < \Delta\Phi_q < -0.15$  [15, 23]). The energy dependences of  $\Delta\Phi_q$  for the largest rapidity interval ( $\Delta y = 3$ ) and for the rapidity interval  $\Delta y = 1.2$  are shown in Fig. 7. A weak decrease of  $\Delta\Phi_q$  with increasing energy is suggested by the data. The numerical values of  $\Delta\Phi_q$  for  $\Delta y = 1.2$  and  $\Delta y = 3$  are given in Table II. Note that the fraction of the accepted tracks for a fixed rapidity interval  $\Delta y$  changes with collision energy, but this alone should not affect  $\Delta\Phi_q$  provided the correlation length is smaller than the acceptance interval in  $y$ .

## VI. DISCUSSION

The study of charge fluctuations in A+A collisions was motivated by the hypothesis that they may be sensitive to the creation of the Quark Gluon Plasma at the early stage

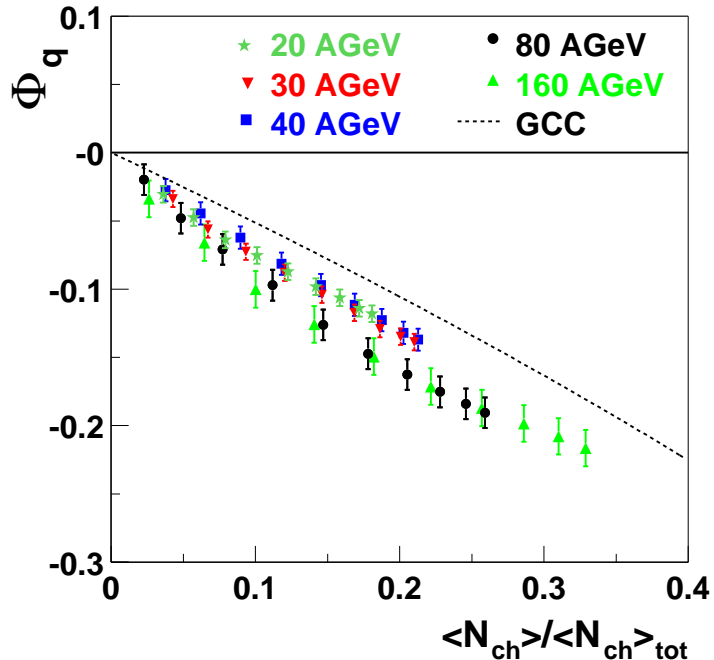


FIG. 5: The dependence of the measure  $\Phi_q$  on the fraction of accepted particles for central Pb+Pb collisions at 20-158 AGeV. Note that experimental points for a given energy are correlated as the data used for a given rapidity interval are included in the broader intervals. The dashed line shows the dependence expected for the case when the only source of particle correlations is the global charge conservation, Eq. 3.

of the collisions. To quantify the expected effect a simple QGP model was proposed in [5]. In this model quarks and gluons are assumed to be in local equilibrium. Assuming entropy and net charge conservation during the evolution from the QGP to the final hadron state in each rapidity interval the number  $N$  of pions and their net charge is calculated. The number of charged pions is taken to be  $N_{ch} = \frac{2}{3} \cdot N$  based on isospin symmetry. Using this model it was shown that the electric charge fluctuations are significantly smaller in the case of QGP creation than in the case of formation of confined matter at the early stage of the collisions (see Fig. 8) [5, 15].

However, this model is not complete. A large fraction of pions originates from decays of resonances [22]. This effect is expected to lead to a distortion of the charge fluctuations established after hadronization. To quantify this effect the model was extended as follows. From the total number of produced final state pions the entropy of the system

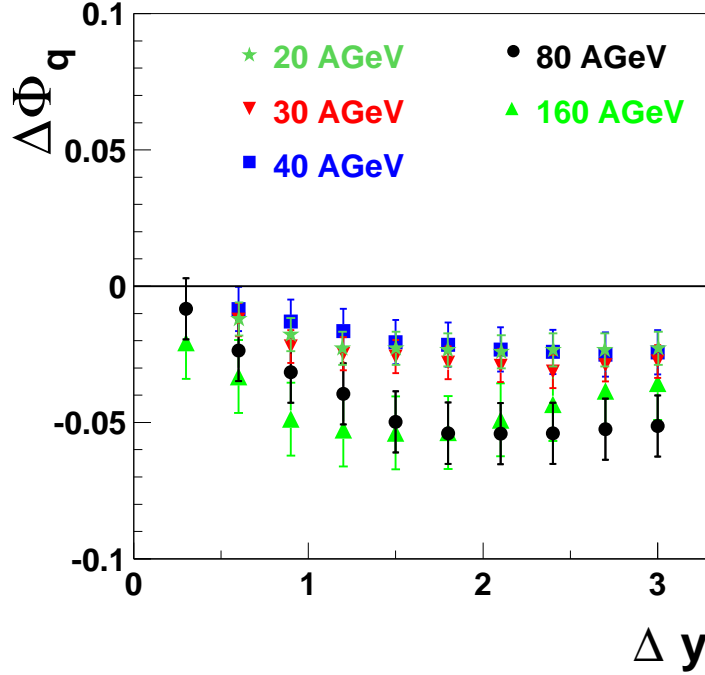


FIG. 6: The dependence of  $\Delta\Phi_q$  on the width of the rapidity interval  $\Delta y$  for central Pb+Pb collisions at 20, 30, 40, 80 and 158 AGeV. Note that experimental points for a given energy are correlated as the data used for a given rapidity interval are included in the broader intervals.

is calculated. This entropy is attributed to the early stage QGP, treated as an ideal gas of massless quarks and gluons. Bose-Einstein- and Fermi-Dirac-statistics are used to calculate equilibrium numbers of quarks and gluons. The rapidity distribution of these partons is centered at  $y = 0$  and is assumed to be of Gaussian shape with  $\sigma = 0.8$ . For the calculations of charge fluctuations the rapidity interval  $-3 < y < 3$  is divided into several (10 and 20) bins and in each bin the entropy and the net-charge of the contained partons is calculated. The resulting values of  $\Delta\Phi_q$  at the QGP level are shown by the dashed line in Fig. 8. In the next step the QGP entropy is attributed to an ideal gas of  $\rho$  mesons. The numbers of  $\rho^+$ ,  $\rho^-$  and  $\rho^0$  mesons in each bin are calculated assuming that  $\frac{1}{3}$  of all  $\rho$  mesons are neutral. Furthermore, all  $\rho$  mesons are assumed to decay into two pions. The rapidity distribution of the pions is divided into 20 bins and the  $\Delta\Phi_q$  is calculated from the number of positively and negatively charged pions in each bin. The results of this model are shown in Fig. 8 by the dotted curve. Note that by construction  $\Delta\Phi_q = 0$  for the full acceptance.

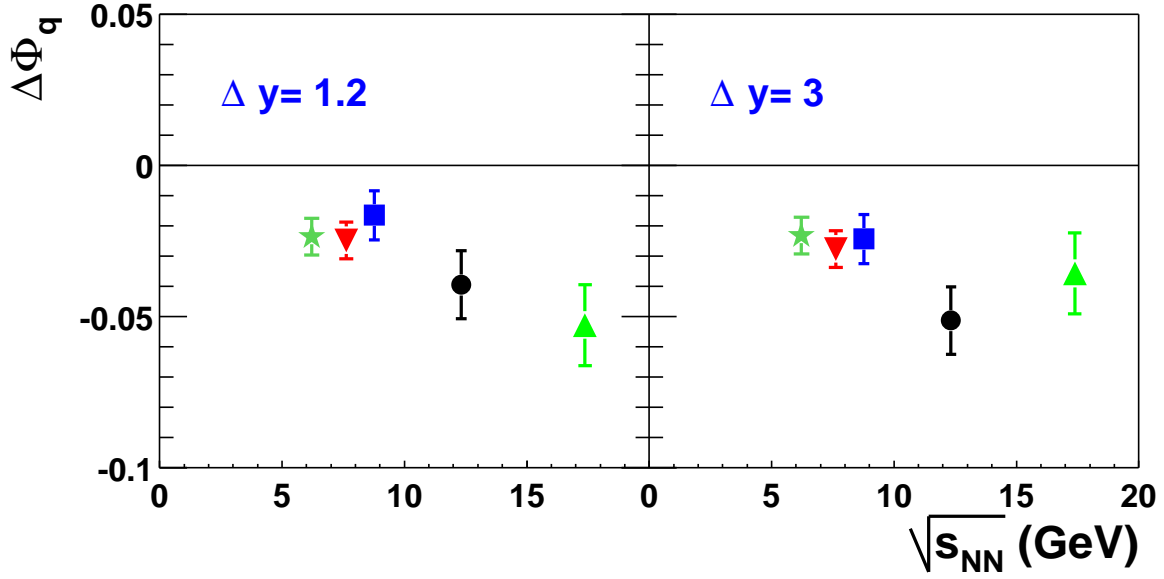


FIG. 7: The energy dependence of  $\Delta\Phi_q$  measured in central Pb+Pb collisions for a narrow rapidity interval  $\Delta y = 1.2$  (left) and a broad rapidity interval  $\Delta y = 3$  (right).

TABLE II: The values of  $\Delta\Phi_q$  for  $\Delta y = 3.00$  and for  $\Delta y = 1.2$  in central Pb+Pb collisions at 20, 30, 40, 80 and 158 AGeV. The first error is systematic, the second statistical.

$\Delta\Phi_q$	20 AGeV	30 AGeV	40 AGeV
$\Delta y = 3$	$-0.023 \pm 0.006 \pm 0.0001$	$-0.028 \pm 0.0003 \pm 0.002$	$-0.024 \pm 0.008 \pm 0.0005$
$\Delta y = 1.2$	$-0.023 \pm 0.006 \pm 0.0001$	$-0.025 \pm 0.0002 \pm 0.016$	$-0.016 \pm 0.008 \pm 0.0003$
$\Delta\Phi_q$	80 AGeV	160 AGeV	
$\Delta y = 3$	$-0.051 \pm 0.011 \pm 0.0002$	$-0.036 \pm 0.013 \pm 0.0003$	
$\Delta y = 1.2$	$-0.040 \pm 0.011 \pm 0.0003$	$-0.053 \pm 0.013 \pm 0.0004$	

As expected, the decays of resonances strongly modify the initial QGP fluctuations. The value of  $\Delta\Phi_q$  increases from values between  $-0.4$  and  $-0.5$  (the lower line in Fig. 8) to values close to zero (the upper line in Fig. 8), the value characteristic for a gas of pions correlated by global charge conservation only. The model demonstrates that the distribution of charged particles in the detector acceptance is strongly distorted by

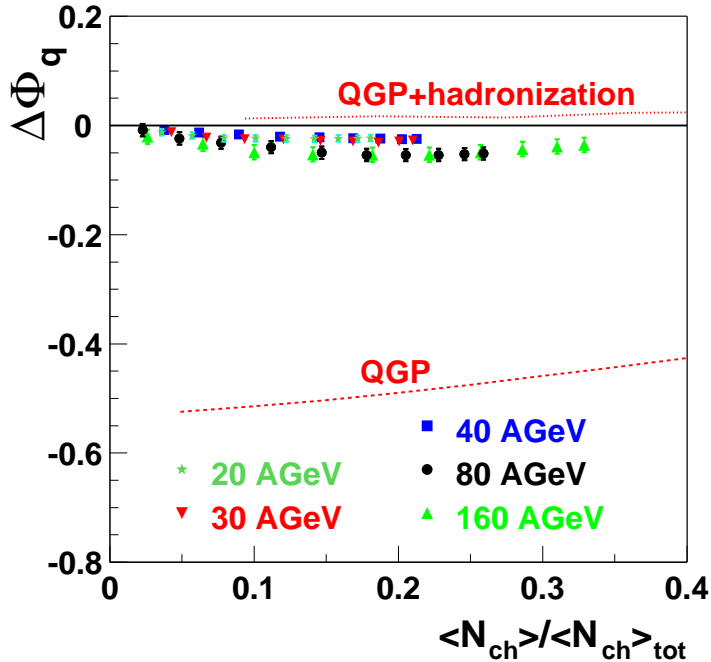


FIG. 8: The dependence of  $\Delta\Phi_q$  on the fraction of accepted particles in central Pb+Pb collisions at 20-158 AGeV. The prediction for the ideal QGP is indicated by the dashed curve (QGP), whereas the prediction for the QGP including hadronization and resonance decay is shown by the dotted curve (QGP+hadronization).

the decay of intermediate resonance states. This may explain why the measurements do not show the suppression of the charge fluctuations naively expected in the case of QGP creation.

The influence of resonance decays on charge fluctuations depends on the size of the rapidity interval  $\Delta y$ , in which fluctuations are calculated. If  $\Delta y$  is much bigger than the typical distance in rapidity of the daughter particles, the charge within the interval will not be changed by the decay and therefore the charge fluctuations should not be affected. On the other hand, if  $\Delta y$  is small, a large fraction of daughter particles will leave the interval and the initial net-charge will be significantly changed. The mean rapidity difference of two pions originating from decays of a  $\rho(770)$  meson is approximately 1 unit of rapidity. Therefore in order to minimize the decay effect the rapidity interval should be much larger than 1. However, this constraint is difficult to fulfill at SPS and lower energies because the rapidity distribution of all produced particles is not much broader



than 1. This explains an approximately constant value of  $\Delta\Phi_q$  calculated within the QGP+hadronization model as seen in Fig. 8. A rapidity interval which is large enough to be unaffected by the influence of resonance decays would contain almost all particles produced in a collision. The net-charge in this interval would then reflect the number of participant protons and the fluctuations would be determined by fluctuations of the collision centrality and not the particle production mechanism. Thus at SPS energies the measured charge fluctuations are not sensitive to the initial QGP fluctuations. At very high energies (when the rapidity distribution of produced particles is significantly broader than 1) the charge fluctuations may be a valid signature of QGP creation.

## VII. SUMMARY

Results on event-by-event charge fluctuations in central Pb+Pb collisions at 20, 30, 40, 80 and 158 AGeV are presented in terms of the  $\Delta\Phi_q$  measure.

The measured  $\Delta\Phi_q$  values are close to zero, as expected for a gas of pions correlated only by global charge fluctuations. This value is significantly higher than that predicted for the creation of a QGP and hadronization into pions with local conservation of entropy and net-charge. A model which incorporates intermediate resonances is described in this paper. Its results show that the decay of  $\rho$  mesons may easily increase the initial QGP charge fluctuations to  $\Delta\Phi_q \approx 0$  thereby completely masking a possible QGP signal at SPS energies.

The slightly negative value of  $\Delta\Phi_q$  indicates correlations between positively and negatively charged particles beyond those from global charge conservation. The origin of these additional correlations may be the final state Coulomb interactions or quantum-statistical effects.

Acknowledgments: This work was supported by the US Department of Energy Grant DE-FG03-97ER41020/A000, the Bundesministerium für Bildung und Forschung, Germany, the Polish State Committee for Scientific Research (2 P03B 130 23, SPB/CERN/P-03/Dz 446/2002-2004, 2 P03B 02418, 2 P03B 04123), the Hungarian Scientific Research Foundation (T032648, T032293, T043514), the Hungarian National Science Foundation, OTKA, (F034707), the Polish-German Foundation, and the Korea Research Foundation Grant

(KRF-2003-070-C00015).

---

- [1] S. V. Afanasiev *et al.* [The NA49 Collaboration], Phys. Rev. C **66**, 054902 (2002) [Axis:nucl-ex/0205002].
- [2] M. Gazdzicki [the NA49 Collaboration], arXiv:nucl-ex/0403023.
- [3] M. Gazdzicki and M. I. Gorenstein, Acta Phys. Polon. B **30**, 2705 (1999) [arXiv:hep-ph/9803462].
- [4] M. I. Gorenstein, M. Gazdzicki and K. A. Bugaev, Phys. Lett. B **567**, 175 (2003) [arXiv:hep-ph/0303041].
- [5] S. Jeon and V. Koch, Phys. Rev. Lett. **85**, 2076 (2000) [arXiv:hep-ph/0003168].
- [6] M. Asakawa, U. W. Heinz and B. Muller, Phys. Rev. Lett. **85**, 2072 (2000) [arXiv:hep-ph/0003169].
- [7] E. V. Shuryak and M. A. Stephanov, Phys. Rev. C **63**, 064903 (2001) [arXiv:hep-ph/0010100].
- [8] K. Adcox *et al.* [PHENIX Collaboration], Phys. Rev. Lett. **89**, 082301 (2002) [arXiv:nucl-ex/0203014].
- [9] J. Adams *et al.* [STAR Collaboration], Phys. Rev. C **68**, 044905 (2003) [arXiv:nucl-ex/0307007].
- [10] C. Blume *et al.*, Nucl. Phys. A **715**, 55 (2003) [arXiv:nucl-ex/0208020].
- [11] H. Appelshauser *et al.* [NA49 Collaboration], Phys. Lett. B **459**, 679 (1999) [arXiv:hep-ex/9904014].
- [12] T. Anticic *et al.* [NA49 Collaboration], arXiv:hep-ex/0311009.
- [13] S. V. Afanasiev *et al.* [NA49 Collaboration], Phys. Rev. Lett. **86**, 1965 (2001) [arXiv:hep-ex/0009053].
- [14] C. Roland [the NA49 Collaboration], arXiv:nucl-ex/0403035.
- [15] J. Zaraneek, Phys. Rev. C **66**, 024905 (2002) [arXiv:hep-ph/0111228].
- [16] C. Pruneau, S. Gavin and S. Voloshin, Phys. Rev. C **66**, 044904 (2002) [arXiv:nucl-ex/0204011].
- [17] S. Mrowczynski, Phys. Rev. C **66**, 024904 (2002) [arXiv:nucl-th/0112007].

- [18] M. Gazdzicki and S. Mrowczynski, *Z. Phys. C* **54**, 127 (1992).
- [19] M. Gazdzicki, *Eur. Phys. J. C* **8**, 131 (1999) [arXiv:nucl-th/9712050].
- [20] S. V. Afanasiev *et al.* [NA49 Collaboration], *Nucl. Instrum. Meth. A* **430**, 210 (1999).
- [21] H. Appelshauser *et al.* [NA49 Collaboration], *Eur. Phys. J. A* **2**, 383 (1998).
- [22] F. Becattini and U. W. Heinz, *Z. Phys. C* **76**, 269 (1997) [arXiv:hep-ph/9702274].
- [23] J. Zaranek, University of Frankfurt, Diploma Thesis (2003).

d)

